On spatially correlated observations in a particle method for subsidence estimation

Samantha S. R. Kim[1*] and Femke C. Vossepoel[1]

[1*]Department of Geoscience and Engineering, Delft University of Technology, Stevinweg 1, Delft, 2628CN, The Netherlands.

*Corresponding author. E-mail: S.S.R.kim@tudelft.nl;
Contributing author: F.C.Vossepoel@tudelft.nl;

Abstract

The particle method is an ensemble-based data assimilation method for state- and parameter estimation in a quasi-static problem. We apply the particle method in two different experiments with models of increasing complexity. The first model, which calculates subsidence for a single observation point due to a single source of strain, considers uncorrelated parameters and observations. In the second model subsidence can be seen as a summation of subsidence contributions from multiple sources. A single source in the second model causes deformation over a region and the observations within this region will be correlated. Assimilating these correlated observations may trigger weight collapse. With synthetic tests we show in a model of subsidence with 50 independent parameters and spatially correlated observations a minimum of $\mathbf{10^{13}}$ particles is required to have information in the posterior distribution identical to that in a model with 50 independent and spatially uncorrelated observations. Spatial correlations cause information loss which can be quantified with mutual information. With synthetic experiments we illustrate how stronger spatial correlation results in a lower information content in the posterior. This quantification underpins our finding that a larger ensemble size is required for the particle method to remain effective in the case of spatial correlation. We furthermore illustrate how this loss of information is reflected in the log likelihood, and how this depends on the number of parameters of the model. Based on the results of these experiments, we propose criteria to evaluate the required ensemble size for data assimilation of spatially correlated fields.

Keywords: Particle method, ensemble size, information theory, weight collapse, subsidence, reservoir.

1 Introduction

The Geosciences, specifically the fields of meteorology, oceanography, physical geography and geophysics, involve the study of complex and nonlinear processes over a range of scales using numerical simulators of varying complexity. Data assimilation is a technique that combines observations with models to estimate model parameters. Complexity of a data assimilation system rapidly increases with the number of parameters in the model and the number of observations, and has implications for how we predict physical processes of the system.

One of the methods used in data assimilation is the particle filter [1] or particle method [2] for static problems. Filtering and ensemble based methods have been applied to subsidence estimation [3, 4] and [5] used ensemble smoother and ensemble smoother multiple data assimilation method to estimate geomechanical parameters of the subsurface. An important question in these applications is whether the ensemble spread is sufficiently large to ensure applicability of the method given the system complexity.

In many applications, the ensemble size is chosen based on trial and error. The particle method, as most other importance sampling methods, suffers from weight collapse and its performance exponentially degrades as the dimension of the state and observation spaces increases [6–8]. We can prevent this weight collapse by increasing the ensemble size. A more systematic approach to evaluate the necessary ensemble size has been proposed by [6] and [7] and tested in a practical example through the work of [9]. However, analytic derivations of the ensemble size in these publications are often based on abstract problems, and thus the results are not always easily translated to geoscience problems. [6] highlight for example the problem of non-Gaussian prior and observations, and the nontrivial dependencies between parameters and observations. In this study, we will extend the results of [6] to empirical cases with observations with spatial correlation, focusing specifically on the feasibility of the particle method and its performance. We illustrate this with an example of subsidence caused by reservoir compaction, where observations of subsidence allow us to estimate geomechanical properties of the reservoir (e.g., [3, 10]).

To assess the feasibility of the particle method to estimate reservoir parameters, we wish to evaluate the required ensemble size to account spatial correlation in the observed field and prevent weight collapse. In a previous study on the particle filter, [6] derive a theoretical relationship between the maximum weight, w_{max} of the particles and the dimension of the problem for an example of i.i.d. (independent identically distributed) samples and under the assumption of a standard normal density for prior and likelihood. In their

study, the authors generalize the results at an asymptotic limit for a case where a linear transformation from model parameters to the observation space can be represented by an I_d (identity) observation operator. Strategies to assimilate spatially correlated observations for large number of observations is developed by [11]. However, to our knowledge, there is no theoretical approach to estimate weight collapse and the required ensemble size when spatial correlation occurs in the observed field. In other words, when the observation operator becomes non-I_d and when the components of the observation vector depend on multiple parameters.

The objective of the present study is to evaluate the necessary ensemble size that ensures the applicability of the particle method and avoid weight collapse as a result of 1) the dimension of the system and 2) on the spatial correlation in the observed field. For this, we use two conceptual models of subsidence: 1) a linear model of subsidence and 2) a multi-component model. In the linear model of subsidence, we use a linear transformation from parameter to observation space to represent a first-order approximation of a compacting reservoir. The multi-component model, that includes spatial correlation, is based on the nucleus of strain approach of [12], which has been used in literature to estimate geomechanical reservoir properties [3, 13]. The resulting subsidence shows spatial correlation, as the field of deformation is a superposition of the strain created by each compacting compartment of the gas reservoir. To extend the derivation of the ensemble size to problems with spatial correlation, we propose an empirical quantification of the information in both prior knowledge and posterior estimate using the formalism of information theory with mutual information.

The paper is organized as follow. In Section 2 we give an overview of the particle method and of the previous results of [6] for weight collapse in high-dimension. Using information theory with the metric of mutual information, we extend the results of [6] to the example of spatially correlated subsidence. Results in Section 5 illustrate how the ensemble size must grow with spatially correlated observations to avoid the efficiency of the particle method to degrade. Sections 6 and 7 conclude our study.

2 The particle method

In this section, we first give an overview of the particle method and the problem of weight collapse, and we introduce the concept of mutual information.

2.1 Background on the particle method

Data assimilation is used to estimate the probability of a model state or parameter $\mathbf{x}$ given the observations $\mathbf{y}$. The particle method that we use in this study is a static application of the particle filter. We consider N_e particles as a Monte Carlo sampling of prior state or parameter $\mathbf{x}$. Each state or parameter in $\{\mathbf{x}_i, i = 1, .., N_e\}$, gives a model representation to be compared with an observation $\{y_i, i = 1, .., N_y\}$, N_y being the number of observations. We define the dimension of the parameter space N_x, and we set the number of observations N_y, equal to the number of parameters: $N_y = N_x$ (e.g., $N_y = N_x = 50$). Model predictions can be described by the observation model,

$$\mathbf{y} = \mathcal{H}\mathbf{x}. \tag{1}$$

Following the formulation of filtering problem in [14], we define the observation operator $\mathcal{H}$. In Eq. 1, the observation operator $\mathcal{H}$ maps the parameters $\mathbf{x}$ to the states $\mathbf{y}$, i.e. observations or model-predicted measurements.

Result of the particle method is a posterior distribution $p(\mathbf{x}|\mathbf{y})$, which takes into account the uncertainties in both model and assimilated observations to evaluates the probability of possible model outcomes. The posterior probability of the model to the observations can be described using Bayes' theorem.

$$p(\mathbf{x}|\mathbf{y}) = \frac{p(\mathbf{y}|\mathbf{x})p(\mathbf{x})}{\int p(\mathbf{y}|\mathbf{x})p(\mathbf{x})d\mathbf{x}}, \tag{2}$$

In Eq. 2 the prior $p(\mathbf{x})$ consists of the ensemble $\mathbf{x}$ sampled from a probability density function. For the parameters $\mathbf{x}$, we compute a model prediction $\mathbf{x^f}$ to map the parameter space to the observation space. The superscript $\mathtt{f}$ stands for "forecast" and represents a prior quantity in the observation space. We later use the superscript $\mathtt{a}$ to refer to the "analysis", or a posterior estimation. We compare the model predictions $\mathbf{x^f}$ with the observations $\mathbf{y}$ through the likelihood $p(\mathbf{y}|\mathbf{x})$. The likelihood is chosen as a probability density function f which represents the distribution and uncertainty in data. In the posterior distribution $p(\mathbf{x}|\mathbf{y})$ each particle is weighted with the likelihoods.

$$w_i = \frac{p(\mathbf{y}|\mathbf{x_i^f})}{\sum_{j=1}^{N_e} p(\mathbf{y}|\mathbf{x_i^f})} \tag{3}$$

In Eq. 3, the posterior weights are normalized with $\sum_{j=1}^{N_e} w_i = 1$. The expected value of the posterior distribution is an estimator of the value of parameters [14]. The quality of the estimator depends on the quality of the posterior and thus on the ensemble size, N_e as well as the dimension of the parameter and observation spaces.

2.2 Weight collapse in the particle method

We define the efficacy of the particle method to estimate model parameters as the ability to get a posterior distribution that represent the prior and likelihood as formulated in Bayes' theorem (Eq. 2). As in any sampling method, the posterior mean becomes a better estimator of the parameters as the number of samples and hence the ensemble size increases.

If a given ensemble size is insufficiently large to sample the prior, we can observe a collapse of the weights in the posterior (Eq. 3). Weight collapse occurs when one single particle has almost all the weight in the estimation of the posterior mean. In this case, the maximum weight, w_{max} of all the particles converges to one. Collapse occurs sooner when the dimensions, N_x and N_y increase, unless the ensemble size increases exponentially as well [7, 8, 15].

Previous results of [6] and [7] give an indication of the applicability of the particle method for a given ensemble size at the asymptotic limit. This asymptotic limit gives the asymptotic condition for collapse for large ensembles and large numbers of observations.

In the following we briefly review the asymptotic theory. For details, we refer the reader to [6] and [7]. The theory of the asymptotic limit is applicable for a case with a prior of state and observation error that are i.i.d. and with an I_d observation operator. As a consequence, we can apply the asymptotic limit to evaluate the ensemble size in a linear model of subsidence without spatial correlation ($\mathcal{H} = I_d$). To compare and understand how weight collapse occurs in a system with spatial correlation, we address the following question:

Can we identify the required ensemble size, and maximum weight w_{max}, for which the particle method is practically applicable?

To derive a theoretical relationship between the required ensemble size, N_e, and the dimension N_y, we start with the assumption of standard normal density for the prior and the likelihood.

To derive this relationship, [6] approximate the likelihood of one particle, $p(\mathbf{y}|\mathbf{x}_i)$, as the product of the likelihoods over the observations, for an I_d observation operator with i.i.d. prior and observation error ϵ.

$$p(\mathbf{y}|\mathbf{x}_i) = \prod_{j=1}^{N_y} f\left[y_j - (\mathcal{H}\mathbf{x}_i)_j\right]. \tag{4}$$

In Eq. 4, for a given observation j, $(\mathcal{H}\mathbf{x}_i)_j$ is the model prediction from the particle x_i seen at the observation point j and f is a standard normal density function $f \sim N(0,1)$. The expression of the likelihood in Eq. 4 can be simplified and expressed as a Gaussian distribution, $N(\mu, \tau)$ by defining a re-scaled mean μ and variance τ.

To do this, we define a log likelihood V_{ij} using $\Psi() = \log f()$ as follows,

$$V_{ij} = -\Psi\left[y_j - (\mathcal{H}\mathbf{x}_i)_j\right], \tag{5}$$

where, using the expression of the log likelihood V_{ij} in Eq. 5, the expression of the likelihood in Eq. 4 can be rewritten as a re-scaled likelihood of $p(\mathbf{y}|\mathbf{x}_i)$

$$p(\mathbf{y}|\mathbf{x}_i) = \exp\left(-\mu - \tau S_i\right). \tag{6}$$

Here, μ is a re-scaled mean and the variance is τ. These are defined as a function of the log likelihood V_{ij}

$$\mu = \sum_{i=1}^{N_y} E(V_{ij}) \qquad \tau^2 = \text{var}\left(\sum_{i=1}^{N_y} V_{ij}\right). \tag{7}$$

An important condition for the expression of the likelihood in Eq. 6 to be a valid approximation of the Eq. 4 is that the scale factor S_i can be approximated by a standard normal density $S_i \sim N(0,1)$. From Eq. 6 and Eq. 7, we express S_i as a function of the log likelihood, μ and τ and later verify its gaussianity with the following expression. S_i is now

$$S_i = \left(\sum_{i=1}^{N_y} V_{ij} - \mu\right)\tau^{-1}. \tag{8}$$

Interestingly, [6] emphasize that in the example of a linear model, the expression of S_i does not directly depend on the parameter dimension, N_x.

Using previous development of the re-scaled likelihood (Eq. 6) and with the approximation $S_i \sim N(0,1)$, we can now connect the maximum weight, w_{max}, to the dimension N_y, and to the ensemble size N_e, in the case of standard normal distribution for the likelihood and the prior. With this, we find

$$E[1/w_{max} - 1] \approx \sqrt{\frac{4}{5}}\sqrt{\frac{\log N_e}{N_y}}. \tag{9}$$

In this expression, the maximum weight, w_{max}, is related to S_i through Eq. 3. [6] use the convergence properties of a $w_{max} \to 1$ and $S_i \sim N(0,1)$ for large N_e and N_y to derive the asymptotic expression (Eq. 9).

Eq. 9 is valid for a Gaussian prior and likelihood under the assumption of S_i converging to a Gaussian distribution.

An important result of [6] is that from Eq. 4 and from the expression of the log likelihood in Eq. 5, the likelihood only depends on the dimension N_y, meaning that the observation dimension, rather than the parameter dimension, controls weight collapse. In case of spatial correlation, the dependencies of the observations to the parameters becomes nontrivial and this may no longer be the case.

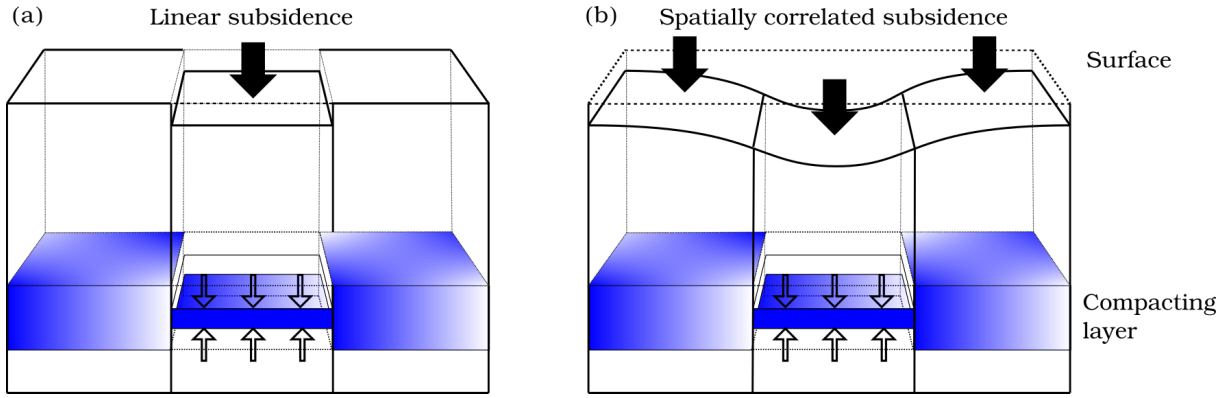

Fig. 1 Models of subsidence. (a) Linear model of subsidence with $\mathcal{H} = I_d$, and (b) the multi-component model of subsidence with spatial correlation. 3D models are built with an ensemble of 1D columns. While the linear model simulates subsidence only for the surface directly above the compartment, the multi-component model computes the deformation field as an integrated response from all compartments.

3 Subsidence models

Subsidence can occur as a consequence of reservoir compaction, which is a decrease in reservoir thickness due a pressure drop, as a result of, for example, gas production. When reservoirs are compartmentalized by faults, some compartments may compact more strongly than others. As a first approximation, we could simulate compaction of a reservoir by simulating the compaction of each reservoir compartment separately. In reality, the total compaction will be the integrated result of the compaction of all compartments. As a simplification, we could simulate the compaction of each compartment separately, without it affecting the surface above other compartments. This is illustrated with respectively the "linear model" and the "multi-component model" in Fig. 1. A commonly used model for subsidence as a result of compaction of a reservoir or reservoir compartment is the nucleus of strain approach of [12, 16, 17]. The nucleus of strain represents compacting reservoir (compartment) as a point source of pressure variation, ΔP. The analytical solution of the vertical deformation at the surface created by a single nucleus of strain

$$u_z(r,0) = \frac{-C_m(1-\nu)V\Delta P}{\pi}\frac{D}{(r^2+D^2)^{3/2}}, \quad (10)$$

where the vertical deformation $u_z(r,0)$ at an observation point is calculated at the surface ($z = 0$) for a nucleus at the depth D with the compaction coefficient of the reservoir, C_m, the Poisson ratio ν and the volume V of the reservoir, the pressure reduction ΔP and the relative position of the nucleus to the observation point.

3.1 Linear model of subsidence

The linear model of subsidence gives a first approximation of reservoir compaction and subsidence and does not take into account the spatial correlation in the subsidence field. To build this

model, we start with a 1D geometrical approximation of subsidence (Fig. 1), and we create adjacent and non-correlated 1D columns of subsurface with Eq. 10. The radial distance r of the nucleus to the observation point is r = 0, such as we have the vertical displacement $u_z(r = 0, 0)$. The number of columns thus indicates the model resolution and the dimension of the parameters and the observation spaces. Because we don't include spatial correlation in the linear model, an observer at one point only sees the compaction in the reservoir compartment directly below (Fig. 1). This model is similar to the example with an I_d observation operator, $\mathcal{H} = I_d$ in [6]. In this subsidence case, $\mathcal{H}$ represents a linear mapping from a vertical compaction of the reservoir to a vertical displacement of the surface.

3.2 Multi-component model of subsidence

The linear model of subsidence computes a local displacement field caused by a single nucleus and the resulting subsidence field does not include the response from the entire compacting reservoir. As an alternative, the nucleus of strain approach is able to model arbitrary shaped reservoirs [16–18] by linearly adding the effect of each nucleus k to the total displacement field

$$\mathbf{u}_z(r, 0) = \sum_{k=1}^{N_x} \mathbf{u}_{z,k}. \tag{11}$$

To evaluate the efficacy of the particle method in more realistic problems, we now incorporate spatial correlation using the multi-component model. Geometry of the multi-component model is similar to the linear model of subsidence. At the reservoir depth, we assume a nucleus of strain in the center of each reservoir compartment and we compute the subsidence (Eq. 10) by calculating the influence of the nucleus of strain over the volume, V, of the reservoir compartment [19]. The difference with the linear model is that the surface displacement u_z at one location j in space arises from all sources of strain in all reservoir compartments (Fig. 1b). The spatial correlation in the multi-component model implies that the observation operator $\mathcal{H}$ is non-I_d. Model-predicted observations are then computed from all components of the vector of parameters. This means that the model $(\mathcal{H}\mathbf{x}_i)_j$ computed for an observation point j with the particle x_i can be written as

$$(\mathcal{H}\mathbf{x}_i)_j = \sum_{k=1}^{N_x} h_{jk} x_{ik}, \tag{12}$$

where h_{jk} is the jk^{th} element of the observation matrix. Recall that the multi-component model integrates the responses of all compartments, and thus is not a one-to-one transformation from parameter space to observation space (i.e., it is a non-injective transformation). This means that in

a multi-component model an observation j is linearly dependent to all $k = 1, ...N_x$ components of the vector of parameters.

In the following, we use these two models to investigate the effect of spatial correlation in weight collapse. The pressure difference, compartment size and thickness are modelled after the Groningen gas reservoir, in the Netherlands (Tab. 1). The mechanical properties are also taken from this reservoir (Tab. 2).

Table 1 Pressure difference, compartment size and thickness of the multi-component model.

	ΔP	dx	dy	dh
Nucleus of strain	-0.35 MPa	0.05°	0.05°	240 m

Table 2 Reservoir properties.

Parameter	Symbol	Value	Unit
Depth	D	2800	m
Thickness	h	240	m
Poisson ratio	ν	0.32	-
Compaction coefficient	C_m	1×10^{-10}	Pa^{-1}

We first test the particle method with the two models of subsidence at the asymptotic limit (Sec. 2.2) and test agreement with the theoretical derivation of weight collapse in the multi-component model. Using concepts from information theory we quantify the available information before assimilation and the information in the posterior to evaluate the required ensemble size in the presence of spatial correlation, i.e., in the multi-component model.

3.3 Synthetic experiments for subsidence models

With synthetic data assimilation experiments, we can assess the efficacy of the particle method to estimate an unknown quantity. To do this we define a "true" value of parameters, $\mathbf{x}^{truth}$ and sample values from this truth to generate synthetic observations for assimilation $\mathbf{y}$, $\{y_i, i = 1, .., N_y\}$ with Eq. 1. The observation operator $\mathcal{H}$ maps the true parameters $\mathbf{x}^{truth}$ to the synthetic observations $\mathbf{y}$. Gaussian noise, ϵ, is linearly added to simulate imperfect observations:

$$\mathbf{y} = \mathcal{H}\mathbf{x} + \epsilon. \tag{13}$$

We use the same observation operator $\mathcal{H}$, as forward modelling operator, to compute the model prediction $p(\mathbf{x}^f)$ from the particles $\mathbf{x}_i$ in Bayes's theorem and to compute synthetic data. We compare the outcome of synthetic experiments with the "true" values of parameters and subsidence estimates as an indication on the efficacy of the particle method.

4 Entropy and mutual information

We investigate weight collapse in data assimilation problems with spatially correlated observations and thus with observable representation of higher

complexity. With the information theory of Shannon [20] which is commonly applied in probability theory in the field of dynamical systems [21]. In information theory, the measure of entropy helps quantify the uncertainty, and conversely the information about an unknown quantity.

[22] demonstrate the use of information theory to diagnose the posterior probability function in Bayesian inverse problems. Although their approach with Shannon's information is not conclusive, they provide insightful perspectives for application of information theory to other methods. [23] further refine the use of entropy and mutual information to evaluate the efficiency of a filtering method. We extend this study to address the problem of weight collapse.

For a particle method, sources of uncertainty are model error, imperfect data and the approximation in the importance sampling algorithm which all propagate into the posterior distribution. The importance sampling algorithm assumes that we can adequately sample the prior. If the sampling is inadequate, for example because of non independent or insufficient samples, weight collapse can occur. In this case, the expected mean of the posterior is no longer a good representation of the true posterior (Eq. 2). This implies a loss of information in the posterior estimate. To evaluate the propagation of information from prior and likelihood to posterior, we use the metric of entropy and mutual information as defined in [24] and [25]. Mutual information allows us to estimate the information about the parameter x contained in the distribution $p(\mathbf{x})$ with respect to an other distribution $p(\mathbf{y})$ (Fig. 2). Using mutual information in data assimilation problems allows us to evaluate the information in both model and data available before assimilation and the ability of the particle method to conserve this information in the posterior.

For a parameter x sampled from a discrete distribution $p(\mathbf{x})$, the entropy $H(x)$ of $p(\mathbf{x})$, can be interpreted as "can we know x given $p(\mathbf{x})$" and is expressed by

$$H(x) = -\sum_i p(x_i) \log\left(p(x_i)\right). \tag{14}$$

The entropy is minimal if the value of the random variable x can be estimated from $p(\mathbf{x})$ with zero uncertainty, meaning that the system is deterministic. Conversely, the entropy is maximum if x can not be estimated from $p(\mathbf{x})$, i.e., $p(\mathbf{x})$ does not provide any information to determine an outcome x. Let us consider the random variables x, y and z. In the synthetic experiments, we have samples of the model predictions, $\mathbf{x^f}$ and we create synthetic observations $\mathbf{y}$ vector for assimilation (Eq. 1). Additionally, in order to apply the metric of [24] we create synthetic observations for validation, $\mathbf{z}$. Both vectors $\mathbf{y}$ and $\mathbf{z}$ have the same dimension,

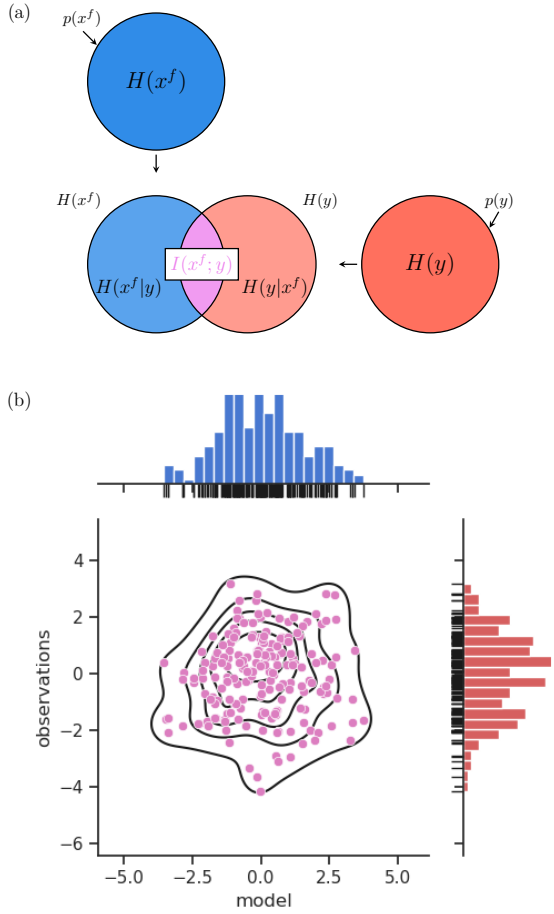

Fig. 2 Venn diagram to illustrate the metric of entropy before assimilation. (a) The colored area in circle represents the entropy of a distribution (e.g. entropy $H(x^{\mathbf{f}})$ of the prior distribution $p(\mathbf{x}^{\mathbf{f}})$). The intersection of the entropy of prior and data constitutes the mutual information $I(x^{\mathbf{f}};\ y)$. The remaining area of entropy (e.g., $H(x^{\mathbf{f}}|y)$) represent the reduced uncertainty on the variable $x^{\mathbf{f}}$ given the knowledge brought by the variable y. (b) The joint probability gives an intuitive approach to mutual information as a measure of similarity between probability distributions. In the example with discrete Gaussian distribution for the prior and the data, if the joint probability shows strong correlation then mutual information increases as the joint probability increases (Eq. 15).

N_y. By construction, observation vectors $\mathbf{y}$ and $\mathbf{z}$ are sampled from the same density, $N(0,1)$, and the same observation model (Eq. 1). We assume them to be independent. $H(x)$ is the entropy in the model and measures the uncertainty on the parameters from the model predictions $\mathbf{x}^{\mathbf{f}}$. Similarly, for the entropy in a data set, we can compute $H(y)$, from observations $\{y_i,\ i = 1,\ ..., N_y\}$.

We can now compute the entropy in model $H(x)$, and in data $H(y)$ with Eq. 14 and the mutual information $I(z;\ x^{\mathbf{f}})$ between $p(\mathbf{z})$ and $p(\mathbf{x}^{\mathbf{f}})$, becomes

$$I(z;\ x^{\mathbf{f}}) = \sum_{z}\sum_{x^{\mathbf{f}}} p(\mathbf{x}^{\mathbf{f}},\mathbf{z}) \log\left(\frac{p(\mathbf{z},\mathbf{x}^{\mathbf{f}})}{p(\mathbf{z})p(\mathbf{x}^{\mathbf{f}})}\right). \tag{15}$$

In Eq. 15, the prior distribution $p(\mathbf{x}^{\mathbf{f}})$, of the model predictions $\mathbf{x}^{\mathbf{f}}$, is then compared with the validation data $\mathbf{z}$, using the joint probabilities $p(\mathbf{z},\mathbf{x}^{\mathbf{f}})$. To compute mutual information, vector model prediction has the dimension of N_y resulting of one model variable $x^{\mathbf{f}}$ per observation site. The joint probability gives the intersection between the model and the observation spaces (Fig. 2). A more practical implementation of mutual information [26], written as a function of the entropy and the joint entropy $H(z,x^{\mathbf{f}})$ is

$$I(z;\ x^{\mathbf{f}}) = H(x^{\mathbf{f}}) + H(z) - H(z,x^{\mathbf{f}}). \tag{16}$$

Also Eq. 16 can be applied to estimate the mutual information $I(z;\ y)$. $I(z;\ x^{\mathbf{f}})$ and $I(z;\ y)$ now give an indication of the information content in the model variable $x^{\mathbf{f}}$ and the assimilated data y, which can be used to evaluate a certain data-assimilation setup. By quantifying propagation

of information content before and after assimilation we can relate weight collapse to particle method performance. We can use this to evaluate the required ensemble size given the model complexity.

To evaluate how the information content before assimilation propagates to the posterior we define differential information I_{diff} and the data assimilation efficiency $\mathcal{E}_{DA}$ [24]. Differential information is the difference between the mutual information in the posterior and in the prior and is expressed as $I_{diff} = I(z : x^{\mathtt{a}}) - I(z : x^{\mathtt{f}})$. This quantity can be negative if the particle method *corrupts* the prior information available before assimilation (e.g., in the model or in the observations). To describe how information from both the prior and observations is conserved in the posterior distribution, we define the data assimilation efficiency $\mathcal{E}_{DA}$. $\mathcal{E}_{DA}$ is the ratio of the posterior mutual information $I(z;\ x^{\mathtt{a}})$ and the prior mutual information $I(z;\ x^{\mathtt{f}}, y)$,

$$\mathcal{E}_{DA} = \frac{I(z;\ x^{\mathtt{a}})}{I(z;\ x^{\mathtt{f}}, y)} \tag{17}$$

The posterior mutual information represents the mutual information between the distribution of the validation data $p(\mathbf{z})$ and the posterior weighted ensemble $p(\mathbf{x}^{\mathtt{a}})$. The prior mutual information $I(z;\ \ x^{\mathtt{f}}, y)$ represents the information available before assimilation and is expressed as a function of the mutual information $I(z;\ x^{\mathtt{a}})$ and of the mutual conditional information $I(z;\ y|x^{\mathtt{f}})$. $I(z;\ \ x^{\mathtt{f}}, y)$ is then the information in the distribution of data $p(\mathbf{y})$ conditioned on the model predictions $p(\mathbf{x}^{\mathtt{f}})$:

$$I(z;\ x^{\mathtt{f}}, y) = I(z;\ x^{\mathtt{f}}) + I(z;\ y|x^{\mathtt{f}}). \tag{18}$$

This conditional information $I(z;\ \ y|x^{\mathtt{f}})$ can be calculated as follows:

$$I(z;\ y|x^{\mathtt{f}}) = \sum_{x^{\mathtt{f}}} \sum_{y} \sum_{z} p(\mathbf{x}^{\mathtt{f}}, \mathbf{y}, \mathbf{z}) \log \left(\frac{p(\mathbf{y}|\mathbf{z}, \mathbf{x}^{\mathtt{f}})}{p(\mathbf{y}|\mathbf{x}^{\mathtt{f}})} \right). \tag{19}$$

For assessment of the efficiency $\mathcal{E}_{DA}$, we use the so-called interaction information $I(x^{\mathtt{f}};\ y;\ z)$:

$$I(z;\ y|x^{\mathtt{f}}) = I(z;\ y) - I(x^{\mathtt{f}};\ y;\ z). \tag{20}$$

Similarly to Eq. 16, to compute the efficiency of the particle method, $\mathcal{E}_{DA}$, we use interaction information as a function of entropy. Posterior entropy $H(x^{\mathtt{a}})$ can be derived from the definition,

$$H(x^{\mathtt{a}}) = -\int p(\mathbf{x}|\mathbf{y}) \log(p(\mathbf{x}|\mathbf{y})) dx dy, \tag{21}$$

with the approximation of

$$p(\mathbf{x}|\mathbf{y}) \ = \ \sum_{i=1}^{N_e} w_i \delta(x - x_i)$$

and the expression of the weight in Eq. 3. A maximum entropy represents a maximum uncertainty on the analysis $x^{\mathtt{a}}$, and likewise a decreasing entropy suggests a decreasing uncertainty. Quantities of mutual information are empirically estimated with histogram estimation methods.

5 Subsidence state- and parameter estimation

5.1 Weight collapse and asymptotic limit for subsidence models

We observe a stronger weight collapse in the case of spatial correlation in the observation field. Figure 3 illustrates weight collapse in the posterior distribution in the subsidence models of this study. The histograms show the distribution of the maximum weight w_{max}, over 1000 simulations for both the linear and the multi-component models of subsidence and for a model dimension of $N_x = [10, 30, 100]$. The maximum weight can be used as an indicator of the particle method performance. It shows that the method performance can rapidly decrease with spatially correlated observations if the ensemble size is inadequate. To evaluate weight collapse in case of spatial correlation and increasing dimension, we test the particle method at the asymptotic limit (Eq. 9). We perform experiments with both the linear and the multi-component

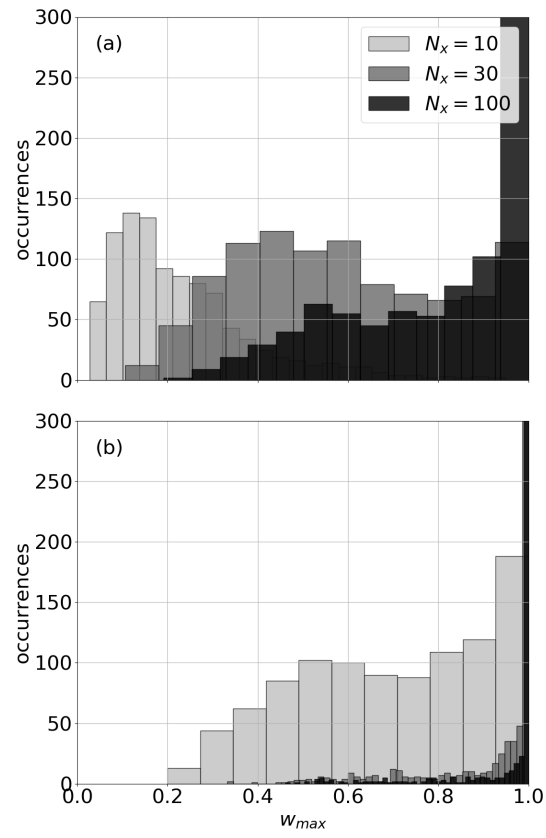

Fig. 3 Maximum weight w_{max} for a linear model of subsidence (a) and for a multi-component model of subsidence with spatial correlation (b) from simulations with, N_x=[10, 30, 100] parameters and an ensemble size $N_e = 1000$. Histograms of w_{max} are computed over 1000 simulations.

models with a large number of observations $N_y = [600, 800, 1000, 1200, 1400, 1600, 1800, 2000]$. In each experiment, we assimilate synthetic observations of subsidence into ensembles with $N_e = N_y^n$ with $n = [0.75, 0.875, 1.0, 1.25]$. Not surprisingly, the results of the linear model (Fig. 4a and b) show a good accordance between simulations and the theoretical prediction of $E[1/w_{max}]$ from Eq. 9. Connecting the maximum weight w_{max}, to the ensemble size N_e, and the number of parameters N_x, through a linear

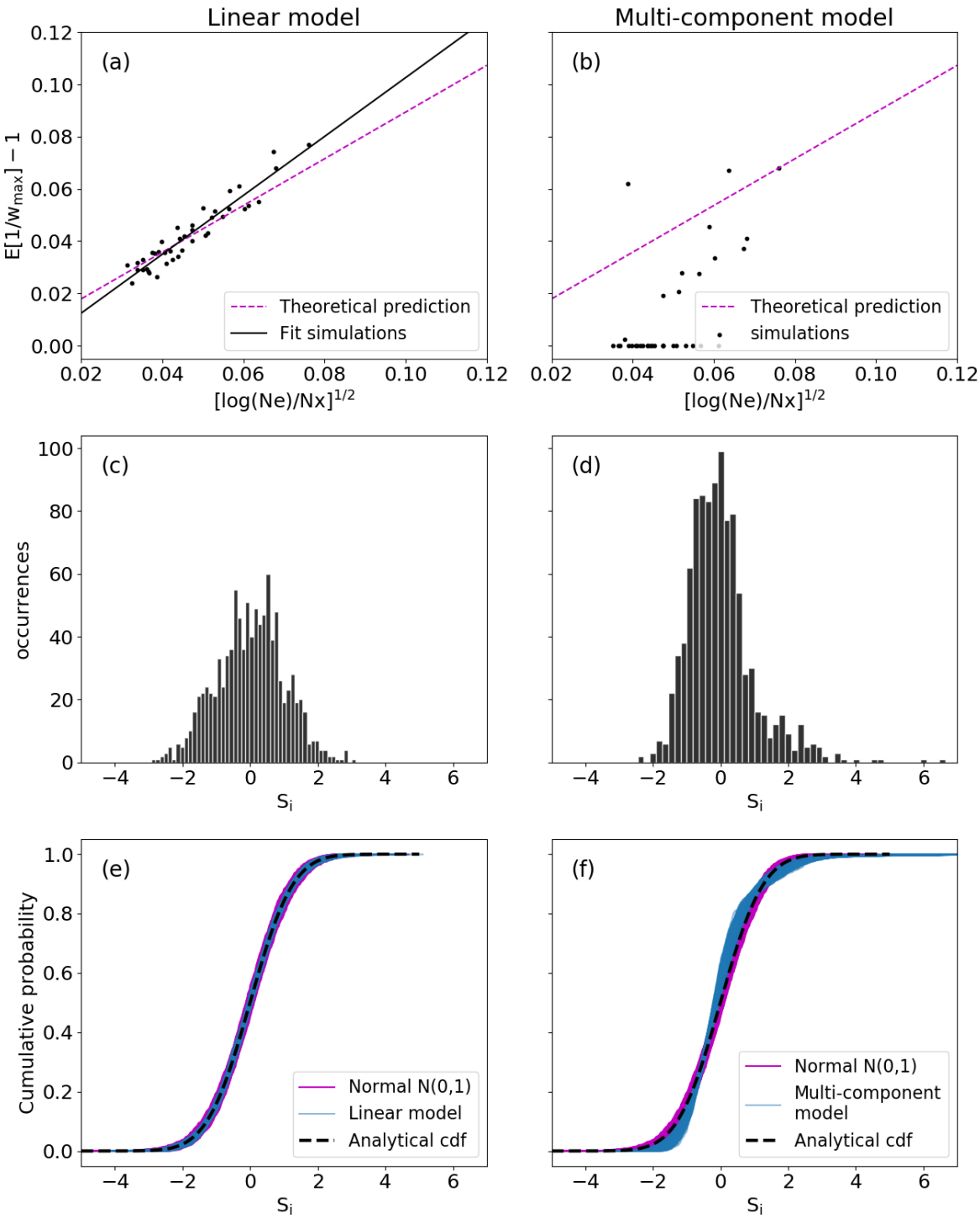

Fig. 4 Results at asymptotic limit for the linear model of subsidence and the multi-component model. Verification of the condition for collapse ((a), (b)). Dashed line gives the theoretical prediction of Eq. 9 and the solid line gives the best fit to the simulations given N_x and N_e. The histograms of the distribution of the scale factor S_i from the re-scaled likelihood in Eq. 8 ((c), (d)). In (e) and (f), Kolmogorv-Smirnov (K-S) tests of the distribution of S_i show the the cumulative probability distributions over 1000 simulations with 1) a sampled standard normal density $N(0,1)$, 2) the subsidence model and in dashed line the analytical cumulative probability of a density $N(0,1)$.

relationship. A linear interpolation of the results suggests that the line of $E[1/w_{max}]-1 = -0.008+ 1.0721\sqrt{\log(N_e)/N_y}$ describes the variability of the maximum weight which exponentially depends on N_e. Particle method in the linear model of subsidence shows good agreement with the results of [6]. However, it clearly appears that the particle method in the multi-component model does not fit the theoretical prediction of Eq. 9. The main difference between the linear model and the multi-component model reflected by the negative log likelihood (Eq. 5) that results from the summation in observation operator $\mathcal{H}$ (Eq. 12). If we assume a Gaussian density for the expression of the negative log likelihood in the linear model

$$V_{ij} \propto \frac{1}{2}\frac{\left[y_i - (\mathcal{H}\mathbf{x}_i)_j\right]^2}{\sigma^2}, \tag{22}$$

this becomes

$$V_{ij} \propto \frac{1}{2}\frac{\left[y_j - x_{ij}^f\right]^2}{\sigma^2}. \tag{23}$$

In the case of spatial correlations, the expression of the negative log likelihood differs as we take into account the linear combinations of parameters (Eq. 12). Because of the mapping from parameter to observation space reflected by $\mathcal{H}$, the log likelihood depends on the parameter dimension N_x (Eq. 24) in the case of spatial correlation. This can be explained by the fact that in the case of spatial correlation, we consider the differences between the vector observation y_j with the states computed from all parameters.

$$V_{ij} \propto \frac{1}{2}\frac{\left[y_j - \sum_{k=1}^{N_x} h_{jk}.x_{ik}\right]^2}{\sigma^2}. \tag{24}$$

To assess how the weight collapse in assimilation with the multi-component model (Eq. 24) differs from the theoretical prediction of weight collapse (Eq. 9), we test the approximation of the observation likelihood in Eq. 6 against the probability distribution of the term S_i in Eq 8. The term S_i is the scale factor which allows us to express the re-scaled likelihood (Eq. 4) as a Gaussian distribution. The main assumption to re-scale this likelihood is on S_i to follow a standard normal density, $S_i \sim N(0,1)$.

The histograms in Fig. 4 show the distributions of S_i in the linear and the multi-component model. The distribution of S_i in the multi-component model shows a skewness compared to result for the linear model, which approaches a standard normal distribution. Distributions of S_i provide evidence of the effect of parameter dependency in Eq. 24 [9].

The histograms in Fig. 4 show the result of S_i for a single simulation. To confirm the deviation to a standard normal density in the distribution of S_i, we perform the K-S (Kolmogorv-Smirnov) tests over 1000 simulations.

The analytical cdf (cumulative density function) of the standard normal distribution and the cdf of sampled distributions from the standard normal density, $N(0,1)$ are first compared to evaluate the spread around the analytical solution (Fig. 4e and f), due to the sampling. For a dimension $N_x = N_y = 1000$ and the ensemble size of $N_e = 1000$, we compute the value of S_i (Eq. 8), and compare to the analytical and sampled cdf. We choose the values of N_x, N_y and N_e to perform simulations of S_i at the asymptotic limit, in a regime where Eq. 9 is valid.

Results in Fig. 4e and Fig. 4f, show a very good overlap of the cdf for the linear model for both the sampled distributions and the S_i distributions. K-S tests confirm the main assumption that S_i is approximately normal in the case of the linear model of subsidence.

The K-S test for the multi-component model exhibits a skewness in the cdf of S_i, in correspondence with the deviation from a standard normal density in the histogram (Fig. 4d). Results with the multi-component model thus suggest that S_i can not always be approximated by a standard normal distribution when the observations are spatially correlated and consequently when the log likelihood explicitly depends on the parameter dimension, N_x in Eq. 24. Implications of non-Gaussian S_i is that 1) the re-scale likelihood in Eq. 6 is not a valid approximation and 2) the relationship between the maximum weight and the required ensemble size is not linear (Fig. 4a and b). With these empirical results, we highlight a limit of the analytical derivation of required ensemble size in a spatially correlated data assimilation problem.

5.2 Entropy and mutual information for subsidence models

We apply the metric of mutual information to evaluate the information content in model, $I(z;\ x^{\mathtt{f}})/H(z)$ and in data $I(z;\ y)/H(z)$ for both the linear and the multi-component model. With synthetic data assimilation experiments, we compute the entropy and mutual information with a histogram method. The sample size in this simulation is the number of model prediction, N_x and the number of observations N_y, respectively for $I(z;\ x^{\mathtt{f}})/H(z)$ and $I(z;\ y)/H(z)$. The bin-width is chosen such that the histogram covers the range of the values of subsidence (e.g., for both model predictions and synthetic observations). For our experiments with the dimension of $N_x = N_y = 50$, sensitivity tests on the robustness of the histogram method led us to choose a bin resolution of 0.5 mm. Table 3 shows

Table 3 Prior information content in model and in data with a bin resolution of subsidence of 0.5 mm and 40 bins for $N_x = N_y = 50$.

	Linear	Multi-component
I(z; $\mathrm{x^f}$)/H(z)	0.76	0.76
I(z; y)/H(z)	0.76	0.77
$\mathrm{I_{tot}}$	0.99	0.99
w_{max} ($N_e = 10^3$)	0.71	0.94

the mutual information for the linear and the multi-component model before assimilation with an information content in model and in data of 0.76. The linear and multi-component model have similar information content before assimilation, which is not surprising, as both have been sampled from the same, Gaussian, distribution. Particle

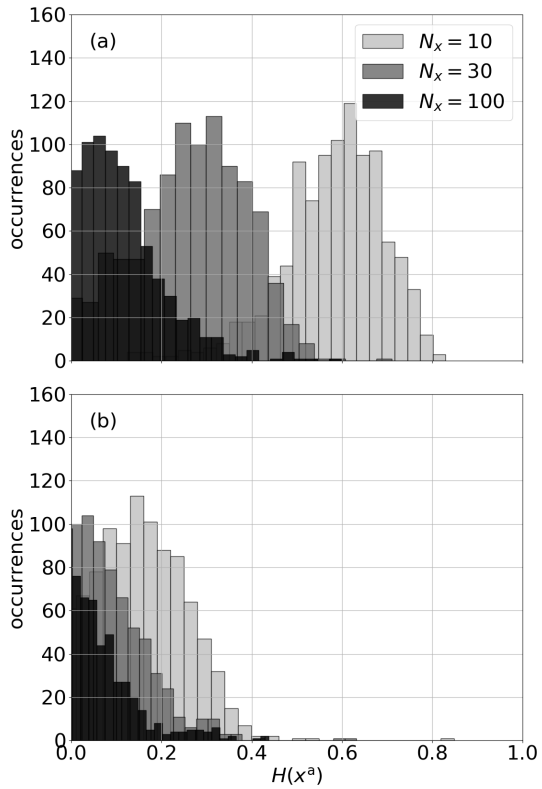

Fig. 5 Posterior entropy for the linear model and the multi-component model of subsidence for the dimension N_x=[10, 30, 100] and 1000 ensemble members. Histograms of entropy (Eq. 14) applied to the weighted posterior probability distribution. Entropy is computed and averaged over 1000 simulations.

method experiments are performed for an ensemble size $N_e = 1000$. As expected from histograms of w_{max} in Fig. 3, weight collapse is stronger in the multi-component model than in the linear model (Tab. 3) as the dimension increases. This suggests that the particle method algorithm itself is the main cause of information loss in the posterior in case of weight collapse. Posterior entropy, $H(x^a)$ in Fig. 5, which represents the uncertainty on the vector of parameters $\mathbf{x}$, after assimilation in the posterior distribution $p(\mathbf{x}|\mathbf{y})$ is computed for the dimensions $N_x = [10, 30, 100]$. Comparing Fig. 5 with Fig. 3, we observe that the posterior entropy decreases as the maximum weight increases. If we compare Fig. 5b with Fig. 5a, posterior entropy converges faster to zero in the case of a model with correlation than in the case of the linear model. The lower entropy suggests a link to weight collapse. Similarly to the maximum weight posterior entropy can be used as a measure of weight collapse (Fig. 3).

5.3 Information content and efficiency

In the following, to evaluate the ability of the data assimilation algorithm to conserve information in the posterior, we use the definitions of the data assimilation efficiency $\mathcal{E}_{DA}$ (Eq. 17), and of differential information I_{diff}. According to the results of information content before assimilation (Tab. 3), we compute $\mathcal{E}_{DA}$ and I_{diff} with the bin-width of 0.5 mm and the dimensions $N_x = N_y = 50$ for an increasing ensemble size N_e. Figure 6

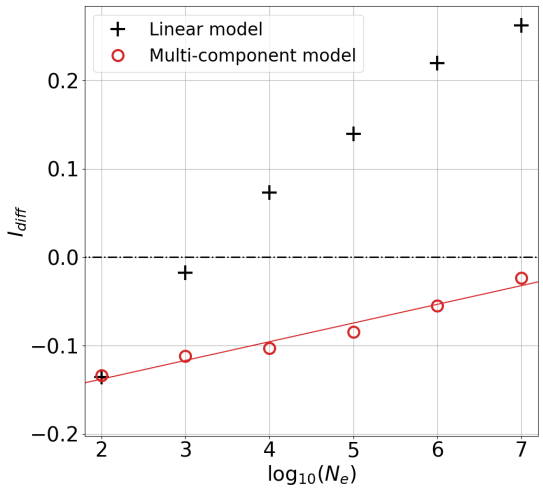

Fig. 6 The differential information I_{diff}, indicates the ability of the posterior to conserve the prior information content. The best fit line of the differential information with the multi-component model is given by $I_{diff} = 0.018 \log_{10}(N_e) - 0.17$.

shows results of I_{diff} for the linear and the multi-component model. Results clearly show a negative I_{diff} for small ensemble size, in agreement with a stronger weight collapse. In the example of the linear model, $I_{diff} < 0$ for ensemble size $N_e < 10^3$ and a maximum weight $w_{max} \sim 0.7$. Differential information increases as a function of the ensemble size N_e, for both the linear and the multi-component model. As expected, the ensemble size of $N_e = 100$ and $N_e = 1000$ are not large enough to avoid weight collapse in the linear model and give a negative differential information I_{diff}. In this example, the information in the posterior distribution is less than in the prior. We refer to this as *corrupted* information with negative differential information. I_{diff} becomes positive for larger ensemble sizes, reflecting an increasing information content in the posterior and a respectively decreasing weight collapse.

Results of differential information with the linear model show good agreement with the estimation of the required ensemble size of [6] and are used as performance benchmark for our study. Transposing this approach to the multi-component model, Fig. 6 shows that with an ensemble size of $N_e = 10^7$ the particle method still corrupts the prior information, with $I_{diff} < 0$ and the maximum weight approaching $\max w_i = 0.8$ (Fig. 7).

To evaluate the ensemble size which preserves the prior information and then ensures the applicability of the particle method in the multi-component model, we compare the efficiency $\mathcal{E}_{DA}$ with the maximum weight and the differential information I_{diff}. The efficiency $\mathcal{E}_{DA}$ as illustrated in Fig. 7 measures the quality of the posterior given the information content in the prior model prediction and the assimilated observations. Comparison of $\mathcal{E}_{DA}$ with the differential information (Fig. 6), shows that the information in the posterior ($\mathcal{E}_{DA} \sim 0.75$) is at least equal to the prior information (Tab. 3) for a positive I_{diff}. An efficiency $\mathcal{E}_{DA}$ larger than the prior information implies that the particle method conserves the prior information content. With the example of the linear model with $N_e = 100$, the particle method does not conserve the prior information with an efficiency of $\mathcal{E}_{DA} = 0.6$ less

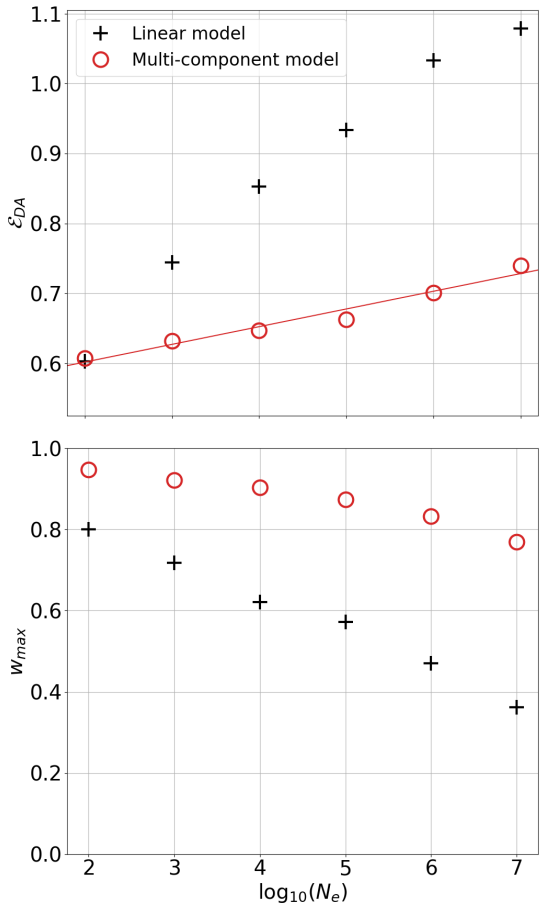

Fig. 7 Efficiency $\mathcal{E}_{DA}$ of the particle method for the linear model and the multi-component model of subsidence for a dimension $N_x = 50$, and with an increasing ensemble size N_e. The best fit of $\mathcal{E}_{DA}$ with the multi-component model is given by $\mathcal{E}_{DA} = 0.022 \log_{10}(N_e) + 0.56$.

than the mutual information before assimilation $I(z;\ x^{\mathbf{f}})/H(z) = 0.76$ (Tab. 3). For an increasing ensemble size $N_e > 10^4$, the particle method now conserves the prior information ($\mathcal{E}_{DA} > 0.75$) and does not *corrupt* the information in the posterior ($I_{diff} > 0$). This result shows that the required ensemble size should be of $N_e > 10^4$, that is consistent again with the previous results of [6]. For equivalent ensemble sizes and equal prior information content, the efficiency in the multi-component model is less than in the linear model. This result confirms that the algorithm of the particle method causes the loss is information when the observations are spatially correlated. For an increasing ensemble size, the efficiency becomes larger than one (Fig. 7a) despite the normalization. This may come from the uncertainty in the histogram method for the calculation of the mutual information. This could be reduced using a sample size larger than $N_x = N_y = 50$ (i.e., model prediction or data).

Using the differential information and the efficiency $\mathcal{E}_{DA}$ we can evaluate a minimum required efficiency of a particle method. We consider an acceptable performance in the linear model for a $\mathcal{E}_{DA}$ at least equal to either the prior information in model or in the observation. Using this approach the differential information has a positive value at $N_e = 10^4$ with the efficiency of $\mathcal{E}_{DA} = 0.85$, which is larger than the prior information content in the model and in the data (Tab. 3). This then suggests $\mathcal{E}_{DA} = 0.85$ as minimum required efficiency corresponding to $I_{diff} > 0.07$ for an ensemble size of $N_e = 10^4$.

In the multi-component model, a linear interpolation in Fig. 7a gives an equivalent performance of $\mathcal{E}_{DA} \sim 0.85$ with an ensemble size larger than $N_e > 10^{13}$. An ensemble size of $N_e > 10^{13}$ is thus required in the example of the multi-component model to have the same performance

as that in a linear model with an ensemble size $N_e = 10^4$. Likewise, the results of I_{diff} in Fig. 6 suggest that we need an ensemble size larger than $N_e > 10^9$ to lift the differential information to a positive value. For I_{diff} to reach ~ 0.07, the required ensemble size should be larger than $N_e > 10^{13}$.

Table 4 Required ensemble size Ne to ensure the particle method applicability in the models of subsidence based on differential information and data assimilation efficiency $\mathcal{E}_{DA}$. Experiments are performed with a bin resolution of subsidence of 0.5 mm and 40 bins for dimensions $N_x = N_y = 50$.

	Linear model	Multi-component model
$I_{diff} > 0$	$N_e > 10^3$	$N_e > 10^9$
$I_{diff} > 0.07$	$N_e > 10^4$	$N_e > 10^{13}$
$\mathcal{E}_{DA} > 0.85$	$N_e > 10^4$	$N_e > 10^{13}$

6 Discussion

Setting an adequate ensemble size can prevent weight collapse in high dimensional problems. Spatial correlation in the observed field increases model complexity and estimation of the required ensemble size can be biased ([6, 7]). In this study, we show in an example with non-I_d observation operator that the requires ensemble size to ensure the applicability of the particle method can increase with spatial correlation.

As in most of the Geoscience systems we use non-injective transformation depending on the strength of the correlations in the observed field, the tendency for weight collapse may vary. Thus, data-assimilation practitioners can expect a possible deviation to the asymptotic results of weight collapse in the linear and Gaussian example. Our empirical results can help derive the required ensemble size. We show that information theory, specifically the metric of mutual information can give empirical criteria to ensure a minimum particle method efficacy. Results of the multi-component model at the asymptotic limit provide insights to understand the deviation from results of particle method with the linear model. In the first part of this study we highlight that in the approximation of the likelihood, the distribution of the scale factor S_i deviates from a standard normal probability distribution. Moreover, the log likelihood explicitly depends on the dimension of the parameter space, N_x, in the case of spatial correlation in subsidence. This could explain why the particle method in the multi-component model suffers of a stronger weight collapse than in the linear model. In the results of [9] at the asymptotic limit with examples of non-linear models, we observed a similar trend at the asymptotic limit in our multi-component model for reservoir models with varying strength of compaction. Our study confirms previous results that the magnitude of weight collapse can vary given the specificity of the problem and the spatial correlation. Evaluating the required ensemble size N_e can be very difficult given model complexity and we highlight the importance of a generalized methodology

to evaluate N_e in Geoscience problems. We propose criteria to evaluate the required ensemble size in Geoscience problems of realistic complexity, involving high dimension and spatial correlation.

Information theory gives a means to quantify the information in the model and in the data and it shows how this information is conserved and propagates in the posterior distribution. We propose a generalized approach to evaluate uncertainty as a *flow of information* for particle methods and other data assimilation methods [23].

The quality of the data assimilation estimate is often assessed with the variance of the posterior distribution or the effective sample size [27, 28]. However, posterior variance can be biased because of weight collapse causing a narrow and non-representative posterior distribution. In our approach, we evaluate the bias caused by weight collapse by assessing the method performance using mutual information though the quantities of differential information and data assimilation efficiency. Differential information I_{diff} and data assimilation efficiency $\mathcal{E}_{DA}$ reveal that weight collapse corrupts the information in the posterior highlighting that the algorithm itself is the main cause of information loss in the posterior

To compute the metric of mutual information we used the histogram method and set the sample size of model predictions and data to $N_x = N_y = 50$ to test the sensitivity of the particle method to the ensemble size N_e. It is important to compare results computed with the same number of parameters, of observations and with the same spread and binwidth in the histogram. The linear model of subsidence provides a benchmark to compare the empirical results of mutual information with theoretical background on weight collapse in the particle filter [6–8, 15]. Results of mutual information show good agreement with previous results of [6]. For this reasons, our methodology with the metric of mutual information could be applied to larger datasets or a time series of data in a filtering and ensemble smoother methods [3, 29]. Weight collapse also occurs in those methods [30].

Usually localization is used to reduce the observation dimension, potentially reducing the information content of a dataset by not taking into account the large scales of spatial correlation. Our approach is of interest for these applications to either assess the method performance (e.g., information loss, ensemble size) or even to optimize the data assimilation before assimilation by evaluating the information content in the prior and in a sample of data. The particle method algorithm could be improved by choosing a more adequate prior proposal [31–34] and using a scheme of resampling methods.

As other criteria to ensure the applicability of particle filter, the maximum weight or an effective sample size of the prior ensemble could be a

threshold to choose the ensemble size and a minimum data assimilation efficacy. However, taken alone it is not clear how we should choose these values. Using a positive differential information I_{diff} and a minimum data assimilation efficiency $\mathcal{E}_{DA}$, one can decide what is the relevant amount of information that the posterior should contain in a specific problem.

7 Conclusion

With an example of models of subsidence we show that the main cause of loss of performance comes from the algorithm itself and only increasing the ensemble size can effectively prevent weight collapse. The required ensemble size in a problem with spatial correlation can be underestimated if evaluated based on non-representative transformation from parameters to observation space. In this study we propose two criteria based on the information theory, differential information and data assimilation efficiency using the metric of mutual information to empirically derive the required ensemble size in case of spatial correlation in the observed field. For this we relate weight collapse and the performance of the particle method to the information content before and after assimilation. We find that in the linear model of subsidence, the particle method requires an ensemble size larger that $Ne > 10^4$ for a dimension $N_x = N_y = 50$ to not corrupt information available before assimilation and to obtain a positive differential information. Our results show good agreement with an earlier study of [6] and provides an empirical method to measure the applicability of a data assimilation method through differential information and the relative (i.e., relative to the prior information) criterion of data assimilation efficiency, to choose the ensemble size. This approach could be further used to track the information content in other data assimilation problems and to optimize the prior information content. Eventually, a careful evaluation of ensemble size could lead to a more reliable use of particle methods.

Acknowledgments

This project is funded by NWO project DEEP.NL.2018.052, “Monitoring and Modelling the Groningen Subsurface based on integrated Geodesy and Geophysics: improving the space-time dimension”. We are thankful to R.F. Hanssen, R. Gover, and G.F. Nane for the valuable discussions and their comments on our manuscript.

References

[1] van Leeuwen, P. J., Künsch, H. R., Nerger, L., Potthast, R. & Reich, S. Particle filters for high-dimensional geoscience applications:

A review. *Quarterly Journal of the Royal Meteorological Society* **145** (723), 2335–2365 (2019). https://doi.org/10.1002/qj.3551 .

[2] Vossepoel, F. C. & van Leeuwen, P. J. Parameter estimation using a particle method: Inferring mixing coefficients from sea level observations. *Monthly weather review* **135** (3), 1006–1020 (2007). https://doi.org/doi.org/10.1175/MWR3328.1 .

[3] Fokker, P., Wassing, B., van Leijen, F., Hanssen, R. & Nieuwland, D. Application of an ensemble smoother with multiple data assimilation to the bergermeer gas field, using ps-insar. *Geomechanics for Energy and the Environment* **5**, 16–28 (2016). https://doi.org/10.1016/j.gete.2015.11.003 .

[4] Zoccarato, C. *et al.* Data assimilation of surface displacements to improve geomechanical parameters of gas storage reservoirs. *Journal of Geophysical Research: Solid Earth* **121** (3), 1441–1461 (2016). https://doi.org/10.1002/2015JB012090 .

[5] Gazzola, L. *et al.* A novel methodological approach for land subsidence prediction through data assimilation techniques. *Computational Geosciences* **25** (5), 1731–1750 (2021). https://doi.org/10.1007/s10596-021-10062-1 .

[6] Snyder, C., Bengtsson, T., Bickel, P. & Anderson, J. Obstacles to high-dimensional particle filtering. *Monthly Weather Review* **136** (12), 4629–4640 (2008). https://doi.org/10.1175/2008MWR2529.1 .

[7] Bengtsson, T., Bickel, P., Li, B. *et al.* Curse-of-dimensionality revisited: Collapse of the particle filter in very large scale systems. *Probability and statistics: Essays in honor of David A. Freedman* **2**, 316–334 (2008). https://doi.org/10.1214/193940307000000518 .

[8] Beskos, A., Crisan, D., Jasra, A. *et al.* On the stability of sequential monte carlo methods in high dimensions. *Annals of Applied Probability* **24** (4), 1396–1445 (2014). https://doi.org/10.1214/13-AAP951 .

[9] Slivinski, L. & Snyder, C. Exploring practical estimates of the ensemble size necessary for particle filters. *Monthly Weather Review* **144** (3), 861–875 (2016). https://doi.org/10.1175/MWR-D-14-00303.1 .

[10] Fokker, P. A., Visser, K., Peters, E., Kunakbayeva, G. & Muntendam-Bos, A. Inversion of surface subsidence data to quantify reservoir compartmentalization: A field study. *Journal of Petroleum Science and Engineering* **96**, 10–21 (2012). https://doi.org/10.1016/j.petrol.2012.06.032 .

[11] Simonin, D., Waller, J. A., Ballard, S. P., Dance, S. L. & Nichols, N. K. A pragmatic strategy for implementing spatially correlated observation errors in an operational system: An application to doppler radial winds. *Quarterly Journal of the Royal Meteorological Society* **145** (723), 2772–2790 (2019). https://doi.org/10.1002/qj.3592 .

[12] Geertsma, J. Land subsidence above compacting oil and gas reservoirs. *Journal of petroleum technology* **25** (06), 734–744 (1973). https://doi.org/10.2118/3730-PA .

[13] Du, J. & Olson, J. E. A poroelastic reservoir model for predicting subsidence and mapping subsurface pressure fronts. *Journal of Petroleum Science and Engineering* **30** (3-4), 181–197 (2001). https://doi.org/10.1016/S0920-4105(01)00131-0 .

[14] Evensen, G., Vossepoel, F. C. & van Leeuwen, P. J. Data assimilation fundamentals: A unified formulation of the state and parameter estimation problem (2022). https://doi.org/10.1007/978-3-030-96709-3 .

[15] Beskos, A., Crisan, D., Jasra, A., Kamatani, K. & Zhou, Y. A stable particle filter for a class of high-dimensional state-space models. *Advances in Applied Probability* **49** (1), 24–48 (2017). https://doi.org/10.1017/apr.2016.77 .

[16] Muñoz, L. F. P. & Roehl, D. An analytical solution for displacements due to reservoir compaction under arbitrary pressure changes. *Applied Mathematical Modelling* **52**, 145–159 (2017). https://doi.org/10.1016/j.apm.2017.06.023 .

[17] Tempone, P., Fjær, E. & Landrø, M. Improved solution of displacements due to a compacting reservoir over a rigid basement. *Applied Mathematical Modelling* **34** (11), 3352–3362 (2010). https://doi.org/10.1016/j.apm.2010.02.025 .

[18] Candela, T. *et al.* Depletion-induced seismicity at the groningen gas field: Coulomb rate-and-state models including differential compaction effect. *Journal of Geophysical Research: Solid Earth* **124** (7), 7081–7104 (2019). https://doi.org/10.1029/2018JB016670 .

[19] Geertsma, J., Opstal, v. *et al.* A numerical technique for predicting subsidence above compacting reservoirs, based on the nucleus of strain concept **30**, 53–78 (1973) .

[20] Shannon, C. *A Mathematical Theory of Cryptography* (1945).

[21] Jost, J. Dynamical systems: examples of complex behaviour (2005). https://doi.org/10.1007/3-540-28889-9 .

[22] Yustres, Á., Asensio, L., Alonso, J. & Navarro, V. A review of markov chain monte carlo and information theory tools for inverse problems in subsurface flow. *Computational Geosciences* **16** (1), 1–20 (2012). https://doi.org/10.1007/s10596-011-9249-z .

[23] Nearing, G. S., Gupta, H. V., Crow, W. T. & Gong, W. An approach to quantifying the efficiency of a bayesian filter. *Water Resources Research* **49** (4), 2164–2173 (2013). https://doi.org/10.1002/wrcr.20177 .

[24] Nearing, G. *et al.* The efficiency of data assimilation. *Water resources research* **54** (9), 6374–6392 (2018). https://doi.org/10.1029/2017WR020991 .

[25] Brewer, B. J. Computing entropies with nested sampling. *Entropy* **19** (8), 422 (2017). https://doi.org/10.3390/e19080422 .

[26] Paninski, L. Estimation of entropy and mutual information. *Neural computation* **15** (6), 1191–1253 (2003). https://doi.org/10.1162/089976603321780272 .

[27] Li, T., Sun, S., Sattar, T. P. & Corchado, J. M. Fight sample degeneracy and impoverishment in particle filters: A review of intelligent approaches. *Expert Systems with applications* **41** (8), 3944–3954 (2014). https://doi.org/10.1016/j.eswa.2013.12.031 .

[28] Martino, L., Elvira, V. & Louzada, F. Effective sample size for importance sampling based on discrepancy measures. *Signal Processing* **131**, 386–401 (2017). https://doi.org/10.1016/j.sigpro.2016.08.025 .

[29] Emerick, A. A. & Reynolds, A. C. Ensemble smoother with multiple data assimilation. *Computers and Geosciences* **55**, 3–15 (2013). https://doi.org/10.1016/j.cageo.2012.03.011 .

[30] Stordal, A. S. & Elsheikh, A. H. Iterative ensemble smoothers in the annealed importance sampling framework. *Advances in Water Resources* **86**, 231–239 (2015). https://doi.org/https://doi.org/10.1016/j.advwatres.2015.09.030 .

[31] Snyder, C. Particle filters, the "optimal" proposal and high-dimensional systems 1–10 (2011) .

[32] Ades, M. & van Leeuwen, P. J. An exploration of the equivalent weights particle filter. *Quarterly Journal of the Royal Meteorological Society* **139** (672), 820–840 (2013). https://doi.org/10.1002/qj.1995 .

[33] Chorin, A. J. & Morzfeld, M. Conditions for successful data assimilation. *Journal of Geophysical Research: Atmospheres* **118** (20), 11–522 (2013). https://doi.org/10.

1002/2013JD019838 .

[34] van Leeuwen, P. J. Particle filtering in geophysical systems. *Monthly Weather Review* **137** (12), 4089–4114 (2009). https://doi.org/10.1175/2009MWR2835.1 .